HHS Public Access

Author manuscript

Nat Struct Mol Biol. Author manuscript; available in PMC 2009 February 01.

Published in final edited form as:

Nat Struct Mol Biol. 2008 August ; 15(8): 805–810. doi:10.1038/nsmb.1466.

The ClC-0 chloride channel is a 'broken' Cl^-/H^+ antiporter

Jiří Lísal and **Merritt Maduke**

Stanford University, Department of Molecular and Cellular Physiology, 279 Campus Drive, Stanford, California 94305, USA

Abstract

Ion channels have historically been viewed as distinct from secondary active transporters. However, the recent discovery that the CLC 'chloride channel' family is made up of both channels and active transporters has led to the hypothesis that the ion-transport mechanisms of these two types of membrane proteins may be similar. Here we use single-channel analysis to demonstrate that ClC-0 channel gating (opening and closing) involves the transmembrane movement of protons. This result indicates that ClC-0 is a 'broken' Cl^-/H^+ antiporter in which one of the conformational states has become leaky for chloride ions. This finding clarifies the evolutionary relationship between the channels and transporters and conveys that similar mechanisms and analogous protein movements are used by both.

Members of the CLC chloride-transport protein family facilitate an impressive array of physiological functions including endocytosis, skeletal muscle excitability, neuronal chloride distribution and epithelial ion transport1–3. This diversity of physiological function is accompanied by a surprising diversity in thermodynamic mechanism. Roughly half of the CLC family members are chloride-selective ion channels, which provide passive pores that allow chloride ions to flow down their electrochemical gradient. The other half are chloride-proton antiporters, which couple protein conformational changes to the stoichiometric exchange of chloride for protons4. To probe the connection between the CLC channels and transporters, we investigated the gating of the ClC-0 chloride channel, the founding member of the CLC family. ClC-0 gating has long been known to be modulated by changes in either intracellular or extracellular proton concentrations5,6. We proposed that, if the mechanisms underlying the CLC ion channels and transporters are similar7, then ClC-0 channel gating may involve coupling to the transmembrane movement of protons rather than mere modulation by protons. Here we exploit the unique gating features of ClC-0 to clearly demonstrate such transmembrane movement of protons.

Correspondence should be addressed to M. M. (maduke@stanford.edu).

AUTHOR CONTRIBUTIONS J. L.
collected the experimental data; J. L. and M. M. designed the experiments, analyzed the data and wrote the manuscript.

Published online at http://www.nature.com/nsmb/

Studies on the ClC-0 channel from the *Torpedo marmorata* electroplax organ have guided our knowledge of CLC channel gating8–10. Ion permeation through the dimeric ClC-0 channel is gated by two separate processes. The first, termed ‘fast gating’, acts on the millisecond timescale, and opens and closes the pore within each subunit of the ClC-0 dimer independently of the other. The second gating process, termed ‘slow gating’, acts on a timescale of seconds and opens and closes both pores simultaneously. This combinatorial gating mechanism results in ClC-0’s characteristic three-level single-channel records, where each of the conductance levels (corresponding to zero, one or two pores open) can interconvert directly to the other two (Fig. 1a–c).

In 1990, Richard and Miller discovered a peculiar asymmetry in ClC-0 channel gating11. They observed that the slow gate closed more frequently from the state with only one pore open (conductance level 1—one fast gate open; one fast gate closed) than from the state with both pores open (conductance level 2—both fast gates open). In contrast, the slow-gate opening proceeded usually to conductance level 2. Thus, cycles 1→0→2→1 (labeled J_+; see an example in Fig. 1b) were substantially more frequent than cycles 1→2→0→1 (labeled J_-; see an example in Fig. 1c). Such asymmetry of the gating cycle violates the principle of microscopic reversibility and demonstrates that the three conformational states are not at thermodynamic equilibrium. Instead, there is a cyclic steady state with net flux around the state diagram (Fig. 1d). According to the second law of thermodynamics, the maintenance of any system in the steady state requires input of external energy to keep the system away from equilibrium. The cycling asymmetry ratio, defined as the ratio of the unidirectional fluxes J_+ and J_-, is limited by the externally delivered free energy ΔG coupled to the cycle of conformational changes:

$$\frac{J_+}{J_-} \leq e^{-\frac{\Delta G}{RT}} \quad (1)$$

where R is the gas constant and T is the absolute temperature12.

Richard and Miller originally suggested that the source of energy driving the gating asymmetry might be the transport of chloride down its electrochemical gradient11. Although this explanation was qualitatively satisfying, it failed to account quantitatively for the data. Specifically, it was found that a transmembrane voltage could power the gating asymmetry at close to the predicted level, but a chloride chemical gradient fell woefully short of the prediction (that is, only the electrical portion of the electrochemical gradient complied with the prediction). Motivated by the recent discovery that a number of the CLC homologs are Cl^-/H^+ antiporters13–15, we tested the possibility that H^+ permeation down its electrochemical gradient drives the gating asymmetry. By analyzing ClC-0 single-channel currents expressed in *Xenopus laevis* oocytes, we show that the proton electrochemical gradient provides all of the energy needed to drive the gating asymmetry. These results support the notion that proton permeation is conserved even in the CLC homologs that are primarily chloride channels.

RESULTS

The proton gradient has a role in driving ClC-0 gating asymmetry

The electrochemical gradient of an ion consists of two parts: (i) the concentration gradient of the ion across the membrane; and (ii) the electrical voltage across the membrane. Whereas the voltage is common for all ions in a given system, the concentrations can be adjusted independently for each ion on both sides of the membrane; therefore, the electrochemical gradient can be controlled independently for each ion.

To directly test the hypothesis that protons have a role in powering the non-equilibrium gating in ClC-0, we manipulated the proton electrochemical gradient and held the chloride electrochemical gradient constant. If the non-equilibrium gating is powered entirely by the chloride electrochemical gradient, then the gating asymmetry should not be affected by this maneuver. Figure 2 shows examples of inside-out patch clamp recordings of single ClC-0 channels that were expressed in *Xenopus* oocytes. Each panel shows the first five asymmetrical slow-gate closures observed in a single patch. The two patches were recorded at the same chloride electrochemical gradient (120 mM symmetrical chloride and −90 mV) but different proton electrochemical gradients. Figure 2a shows the patch recorded with a one-pH-unit gradient (internal pH (pH_{int}) 7.5, external pH (pH_{ext}) 8.5). In this case, the overall proton electrochemical gradient is inward (movement of protons from the extracellular to the intracellular side is energetically downhill) because the effect of the transmembrane voltage predominates over the effect of the outward pH gradient according to the equation:

$$\Delta G_H = RT\ln\frac{[H^+]_{\text{int}}}{[H^+]_{\text{ext}}} + FV \quad (2)$$

The patch shown in Figure 2b was recorded with a two-pH-unit gradient (pH_{int} 7.0, pH_{ext} 9.0). This pH gradient overwhelms the negative voltage and makes the overall proton electrochemical gradient outward. In Figure 2a, we observe a strong gating asymmetry, with all five slow-gate events displaying a cycle in the J_+ direction (entering the slow-inactivated state with one pore open and returning with both pores open). In contrast, in Figure 2b, the asymmetry is lost, with three events displaying a cycle in the J_- direction and only two in the J_+ direction.

The only difference between the patch recording conditions in Figure 2a and Figure 2b is the pH; in particular, the direction of the proton electrochemical gradient changes from inward to outward. Because the Cl^- concentrations remain unchanged, the observed decrease in gating asymmetry cannot arise solely from the chloride electrochemical gradient, and thus the proton electrochemical gradient must have an important role in ClC-0 gating. However, a result obtained from a single patch is not statistically reliable because of the low number of the slow-gate closures occurring within a lifetime of the patch. Therefore, we pooled data from several patches, calculated the accumulated gating asymmetry ratio J_+/J_- and estimated 95%-confidence intervals (Methods).

The chloride gradient is not sufficient to drive the asymmetry

To carefully scrutinize the previous proposal that chloride movement powers the gating asymmetry, we eliminated any influence of proton transport on our results by applying a one-pH-unit gradient across the membrane while recording currents at a transmembrane voltage of −58 mV. Under these conditions, the energy of the proton chemical gradient offsets the energy of the electrical potential, and the net proton electrochemical potential gradient is zero. Hence, the free energy obtained from proton transport across the membrane, ΔG_H, is zero. Any gating asymmetry observed would therefore have to be driven by chloride transport down its electrochemical gradient.

The chloride electrical gradient is given by:

$$\Delta G_{Cl} = -RT\ln\frac{[Cl^-]_{int}}{[Cl^-]_{ext}} + FV \quad (3)$$

Recordings with equal chloride concentrations on the two sides of the membrane, which should show a gating asymmetry ratio close to 10 if the non-equilibrium gating is powered by chloride transport (equation (1)), yielded a gating asymmetry ratio J_+/J_- of only 1.9 (95%-confidence interval: 0.8–4.3; Fig. 3a and Table 1). Similarly, recordings with a ten-fold difference in chloride concentration between the two sides of the membrane, which should give an even higher gating asymmetry ratio of close to 100 if the non-equilibrium gating is powered by the chloride transport (equation (1)), again yielded an asymmetry ratio close to unity, $J_+/J_- = 2.6$ (95%-confidence interval: 1.0–7.0; Fig. 3a and Table 1). These results contest the previous hypothesis that chloride transport is responsible for ClC-0 non-equilibrium gating.

Proton transport quantitatively accounts for the asymmetry

Next, we quantitatively tested the gating asymmetry at several nonzero values of the proton electrochemical gradient. This was achieved using different voltages and different pH gradients across the membrane (Table 1). At negative values of ΔG_H (that is, at inward driving force for protons), a transmembrane voltage alone (Fig. 3b, black symbols) or in combination with a pH gradient (Fig. 3b, red symbols) drove the gating asymmetry according to our prediction (based on equation (1)). These data clearly demonstrate that the energy released from inward proton transport down the electrochemical gradient powers the ClC-0 non-equilibrium gating. At positive values of ΔG_H (that is, at outward driving force for protons), on the basis of thermodynamics we expected that the gating asymmetry would proceed in the opposite direction (that channels would enter the slow-gate inactivated state with both pores open and would return with one pore open). However, we found rather that the gating asymmetry simply faded away, and the J_+/J_- ratio leveled at 1 (Fig. 3b, blue symbols). Thus, the mechanism powering the gating asymmetry is unidirectional.

DISCUSSION

Our data indicate that the proton electrochemical gradient provides the energy for the asymmetrical gating of ClC-0. To power the non-equilibrium gating, protons must

completely traverse the membrane—no energy is generated if protons move partially across the membrane and then back out the same side. Thus, the process of ClC-0 gating must involve proton transport. This signifies that ClC-0 combines features of both a passive ion channel (high-throughput chloride conductance) and an active secondary transporter (coupling of protein conformational changes to movement of protons across the membrane). A simple explanation is that the ancestral form of ClC-0 was a Cl^-/H^+ antiporter, as are many of ClC-0's modern-day homologs13–15, and that later in evolution a conformational state of one of the CLC proteins became leaky for chloride ions, thus turning the protein into a chloride channel that still transports protons.

How might the proton transport be coupled to ClC-0 gating? Results from previous studies provide central elements that we will use in proposing a potential mechanism. First, it is well known that ClC-0 fast gating is regulated by protons. Lowering the intracellular pH shifts the voltage-activation curves leftward6. Thus, activation by intracellular protons is voltage dependent. Lowering the extracellular pH also activates, but does so through a different mechanism, increasing the minimal open probability at negative voltages5. This process has little voltage dependence. Recently, a conserved glutamate has been fingered as the residue responsible for conferring sensitivity to both extracellular and intracellular protons7,16. This conserved glutamate has also been identified as the physical 'gate' that blocks chloride permeation during fast gating. Neutralization of this glutamate by mutation or protonation causes the side chain to swing out of the way, opening the channel's chloride permeation pathway5,17. Altogether, this work on the pH dependence of ClC-0 fast gating reveals that the conserved glutamate (the 'glutamate gate') has a central role, and that movement of this glutamate out of the chloride permeation pathway is catalyzed by protonation from either the extracellular or intracellular solutions.

A second element contributing to our proposed mechanism is the structure of the ClC-ec1 antiporter. Our use of this structure is justified on the basis of previous studies that show that it is a reliable guide for mapping various regions of ClC-0, including the pore18–20. Our primary use of the structure will be to identify the position of the glutamate gate residue. The glutamate gate residue in ClC-ec1 has a similar role to that in ClC-0: it blocks the chloride permeation pathway and is essential for proton dependence17,21. Given this similarity, we are confident in positioning this residue near the extracellular side of the protein in ClC-0, similarly to where it is located in ClC-ec1. This positioning fits nicely with the data on ClC-0 mentioned above: it makes sense that protonation of an extracellular residue would be voltage dependent when the proton comes from the inside, and would have little voltage dependence when the proton comes from the outside. Our secondary use of the ClC-ec1 structure is to demark the chloride and proton permeation pathways. In ClC-ec1, the chloride permeation pathway is defined by the chloride ions seen in the structure; this pathway is preserved in ClC-0 (refs. 18,19). The proton permeation pathway is thought to coincide with the Cl^- pathway at the extracellular side and diverge as it moves toward the cytoplasm21. Although there are yet no data identifying residues involved in proton permeation through ClC-0, we propose that, given the other similarities between ClC-ec1 and ClC-0, the assumption that the proton pathways are similar is a reasonable starting point.

The final element in our proposed mechanism is the observation that the slow gate is modulated by protons6,10. Although the mechanistic details of the modulation have not been studied in depth, a clue to the strong coupling between fast and slow gating is provided by the observation that mutation of the fast-gate glutamate abolishes the slow gating16. The key piece of information we will use in our model is that slow-gate opening (similarly to the fast-gate opening) is activated by protonation from either the extracellular or intracellular side.

A model for a possible proton-coupling mechanism in ClC-0 gating can now be described. In the diagram illustrating this model (Fig. 4), the chloride- and proton-translocation pathways in ClC-0 take similar trajectories to those proposed for ClC-ec1. To fit our data, three simple assumptions need to be made. First, the extracellularly located fast gate (at the location of the glutamate gate residue) controls not only chloride permeation, but also proton permeation in a way that protons (similarly to chloride) can pass through the gate only when open. Second, there is a proton binding site toward the intracellular side. Protons from the outside can bind to this site only when the fast gate is open, whereas protons from the inside can bind regardless of the state of the fast gate. Third, protonation of this intracellular site increases the probability of slow-gate opening (Fig. 4, above) and deprotonation decreases the probability of slow-gate opening (Fig. 4, below). When only one subunit of the dimer is protonated the slow gate adopts either conformation equally (Fig. 4, middle). These three simple assumptions lead to the observed cycling of the ClC-0 channel. With an inwardly directed proton-driving force (Fig. 4), the slow gate opens more frequently when the fast gates are open because this allows the protons to enter and bind, and it closes when the fast gates are closed because the protons escape down their electrochemical gradient.

This model also explains why we observe cycling in only one direction. When the proton-driving force is outward, protons enter the binding site from the intracellular side and therefore can bind and unbind independently of the state of the extracellularly located fast gate. As a result, the slow gate is not coupled to the fast gate, and the gating asymmetry ratio equals to unity as observed. Thus, this simple scheme can simulate the observed gating asymmetry and provides a possible mechanism for coupling proton transport to channel gating.

In this model, the ‘fast-gating proton’ and the ‘slow-gating proton’ (the proton that is transported) are two different protons. The fast-gating proton binds and unbinds to the gating glutamate with the frequency of the fast-gate opening and makes the fast gate open and close. When this fast-gating proton is bound to the gating glutamate and the fast gate is open, another proton (the slow-gating proton) slips through the open fast gate and is transported to the second protonation site, opening the slow gate. Such a model is necessary to fit the observed gating asymmetry data: if the fast-gating protons were transported directly to the second protonation site, the fast gate would subsequently close, and we would not see the channel’s preference for opening the slow gate when the fast gates are open. We propose that this might be the point where the antiporter is ‘broken’. We suggest that in the real antiporter only one proton is involved in the ion-exchange cycle. This proton first binds to the external gating glutamate and opens the external gate letting two bound chloride ions out. Subsequently, the proton unbinds from the gating glutamate and is transported deeper to

the second protonation site. Here its binding opens the intracellular gate and allows another two chlorides to bind inside the antiporter. Finally, the proton is released into the cytoplasm. In contrast, in the channel when the first proton is bound to the external gate, another proton can slip through the gate and get to the second protonation site, making the intracellular (slow) gate open at the same time. Thus, in the channel, both gates can be open at the same time, and the ions (both chloride and protons) can flow freely (albeit at very different rates from one another). Although the specific details of this mechanism and the identity of the residues involved remain to be determined, this model provides a basic framework for understanding the proton-coupled gating asymmetry in ClC-0.

To supply energy for the gating asymmetry, transport of even a single proton per one slow-gate inactivation episode is sufficient. For ClC-0, under typical conditions, this would result in a proton flux on the order of 1 s^{-1}, which is too low to be detected by conventional methods, and therefore the experiments presented here may be the only way to uncover the proton transport. In contrast to ClC-0, the slow gate of ClC-0's human ortholog, ClC-1, operates on the millisecond timescale22,23, and indeed a measurable proton flux through ClC-1 was found previously14. Such a flux may be physiologically relevant, for example, in modulating the changes in cytoplasmic pH that occur during muscle activity24. If a similar mechanism of gating-mediated proton transport occurs in the other CLC chloride channels, then the physiological proton electrochemical gradients may influence their roles in epithelial and neuronal settings1.

The 'broken transporter' mechanism for ClC-0 restores a satisfying unity to the CLC family. Until now, the family has seemed divided between two major classes of membrane proteins, channels and secondary active transporters. Secondary active transporters work by coupling protein conformational changes to the stoichiometric movement of ions, whereas channels provide an open pore that allows ions to flow down (and only down) their electrochemical gradient4. To prevent this free diffusion and maintain strict coupling stoichiometry, CLC family members of the antiporter subtype must possess two gates. Although the mechanisms of CLC antiporter gating are not as well understood as those underlying channel gating, it is tempting to speculate that the conformational changes underlying fast and slow gating in ClC-0 parallel the conformational changes in the two gates of the antiporters. However, in studies thus far, the antiporter subunits seem to act independently, and there is no evidence for a large cooperative conformational change such as the one observed in slow gating25,26. Nevertheless, it is possible that cooperativity on a more subtle level will be revealed once the mechanism of the antiporters is understood in greater detail.

By demonstrating that the ClC-0 chloride channel couples the conformational changes of channel gating to the movement of protons, we have revealed a channel behaving like a transporter. This affirms the hypothesis that the unusual features of ClC-0 channel gating are a remnant of transporter activity7 and that proton permeation must be included in any future model of the ClC-0 gating mechanism7,16. Our results add to the growing body of evidence in which the distinction between channels and transporters is blurred, including the recent discoveries of transporters with channel-like properties27,28 and channels with transporter homologs13. The mechanistic interpretations of these findings are not yet fully understood, in part because channel mechanisms in general have been more thoroughly worked out than

transporter mechanisms. The CLC family provides an important prototype for unraveling the relationship between channel and transporter mechanisms: X-ray crystallographic studies provide a high-resolution structural foundation for this family17; electrophysiological studies add a solid mechanistic understanding of the ion-channel mechanisms8,29,30; and our present results provide a crucial connection to the antecedent anti-porter mechanism.

METHODS

Single-channel recordings

We injected *X. laevis* oocytes with 0.03–0.3 ng of the RNA encoding ClC-0 from *T. marmorata*31 and incubated them at 17 °C for 4–8 d before recording. We selected only oocytes with whole-cell ClC-0 currents in the range of 2–5 μA at +50 mV and recorded single channels from inside-out patches at 21 ± 1 °C. The bath solution (intracellular side of the patch) was composed of 110 mM *N*-methyl-*D*-glucamine (NMDG), 110 mM HCl, 5 mM $MgCl_2$, 1 mM EGTA, 10 mM HEPES, pH 7.50, adjusted by NaOH. The pipette solution (extracellular side of the patch) had the same composition at pH 7.50 and differed only in the buffer compounds at other pH values (10 mM 2-(*N*-cyclohexylamino)ethane sulfonic acid (CHES) for pH 9.50; 10 mM Tris for pH 8.50). For measurements with asymmetrical chloride concentrations, the pipette solution contained 110 mM NMDG, 2 mM HCl, 108 mM glutamic acid, 5 mM $MgCl_2$, 1 mM EGTA, 10 mM Tris, pH 8.50. Single-channel currents were sampled at 5 kHz and low-pass filtered at 200 Hz.

Data analysis

Data used for analysis were confined to $pH_{ext} > 6.5$ because missed events led to uncertainties in the J_+/J_- ratio estimation at lower pH. To discriminate between the fast-gate and the slow-gate closures we constructed histograms of the closed-state durations (Supplementary Fig. 1 online). The fast-gate closures were identified by a fit-to-exponential distribution; events falling significantly outside this distribution were assigned as slow-gate closures. Owing to a limited lifetime of the patches, data collected from many patches were pooled together (Table 1). 95%-confidence intervals of the gating asymmetry ratios J_+/J_- were calculated as follows, using the NIST/SEMATECH e-Handbook of Statistical Methods (http://www.itl.nist.gov/div898/handbook/):

$$\text{Lower limit} = \frac{\frac{\chi^2_{\alpha/2}}{2} + J_+ - A}{\frac{\chi^2_{\alpha/2}}{2} + J_- + A} \quad (4)$$

$$\text{Upper limit} = \frac{\frac{\chi^2_{\alpha/2}}{2} + J_+ + A}{\frac{\chi^2_{\alpha/2}}{2} + J_- - A} \quad (5)$$

where

$$A = \chi_{\alpha/2} \sqrt{\frac{J_+ J_-}{J_+ + J_-} + \frac{\chi^2_{\alpha/2}}{4}} \quad (6)$$

and the coefficient $\chi_{\alpha/2} = 1.96$.

Supplementary Material

Refer to Web version on PubMed Central for supplementary material.

Acknowledgments

We thank K. Matulef for help with the data analysis and R. Blaustein, B. Kobertz, R. Lewis, R. Reimer, J. Huguenard and members of the Maduke laboratory for comments on the manuscript. This work was supported by the US National Institutes of Health grant R01 GM070773 and by the Mathers Foundation. J. L. is supported by the Human Frontiers Science Program.

References

1. Jentsch TJ, Poet M, Fuhrmann JC, Zdebik AA. Physiological functions of CLC Cl^- channels gleaned from human genetic disease and mouse models. Annu Rev Physiol. 2005; 67:779–807. [PubMed: 15709978]
2. Puljak L, Kilic G. Emerging roles of chloride channels in human diseases. Biochim Biophys Acta. 2006; 1762:404–413. [PubMed: 16457993]
3. Sile S, Vanoye CG, George AL Jr. Molecular physiology of renal ClC chloride channels/transporters. Curr Opin Nephrol Hypertens. 2006; 15:511–516. [PubMed: 16914964]
4. Stein, WD. An Introduction to Membrane Transport. Academic; San Diego, CA: 1990. Carriers and Pumps.
5. Chen MF, Chen TY. Different fast-gate regulation by external Cl^- and H^+ of the muscle-type ClC chloride channels. J Gen Physiol. 2001; 118:23–32. [PubMed: 11429442]
6. Hanke W, Miller C. Single chloride channels from *Torpedo* electroplax. Activation by protons. J Gen Physiol. 1983; 82:25–45. [PubMed: 6310023]
7. Miller C. ClC chloride channels viewed through a transporter lens. Nature. 2006; 440:484–489. [PubMed: 16554809]
8. Chen TY. Structure and function of CLC channels. Annu Rev Physiol. 2005; 67:809–839. [PubMed: 15709979]
9. Dutzler R. The ClC family of chloride channels and transporters. Curr Opin Struct Biol. 2006; 16:439–446. [PubMed: 16814540]
10. Matulef K, Maduke M. The CLC 'chloride channel' family: revelations from prokaryotes. Mol Membr Biol. 2007; 24:342–350. [PubMed: 17710638]
11. Richard EA, Miller C. Steady-state coupling of ion-channel conformations to a transmembrane ion gradient. Science. 1990; 247:1208–1210. [PubMed: 2156338]
12. Hill, TL. Free Energy Transduction in Biology. Academic; New York, NY: 1977.
13. Accardi A, Miller C. Secondary active transport mediated by a prokaryotic homologue of ClC Cl^- channels. Nature. 2004; 427:803–807. [PubMed: 14985752]
14. Picollo A, Pusch M. Chloride/proton antiporter activity of mammalian CLC proteins ClC-4 and ClC-5. Nature. 2005; 436:420–423. [PubMed: 16034421]
15. Scheel O, Zdebik AA, Lourdel S, Jentsch TJ. Voltage-dependent electrogenic chloride/proton exchange by endosomal CLC proteins. Nature. 2005; 436:424–427. [PubMed: 16034422]
16. Traverso S, Zifarelli G, Aiello R, Pusch M. Proton sensing of ClC-0 mutant E166D. J Gen Physiol. 2006; 127:51–65. [PubMed: 16380443]

17. Dutzler R, Campbell EB, MacKinnon R. Gating the selectivity filter in ClC chloride channels. Science. 2003; 300:108–112. [PubMed: 12649487]
18. Chen MF, Chen TY. Side-chain charge effects and conductance determinants in the pore of ClC-0 chloride channels. J Gen Physiol. 2003; 122:133–145. [PubMed: 12885875]
19. Engh AM, Maduke M. Cysteine accessibility in ClC-0 supports conservation of the ClC intracellular vestibule. J Gen Physiol. 2005; 125:601–617. [PubMed: 15897295]
20. Estevez R, et al. Conservation of chloride channel structure revealed by an inhibitor binding site in ClC-1. Neuron. 2003; 38:47–59. [PubMed: 12691663]
21. Accardi A, et al. Separate ion pathways in a Cl^-/H^+ exchanger. J Gen Physiol. 2005; 126:563–570. [PubMed: 16316975]
22. Saviane C, Conti F, Pusch M. The muscle chloride channel ClC-1 has a double-barreled appearance that is differentially affected in dominant and recessive myotonia. J Gen Physiol. 1999; 113:457–468. [PubMed: 10051520]
23. Accardi A, Pusch M. Fast and slow gating relaxations in the muscle chloride channel CLC-1. J Gen Physiol. 2000; 116:433–444. [PubMed: 10962018]
24. Aickin CC. Intracellular pH regulation by vertebrate muscle. Annu Rev Physiol. 1986; 48:349–361. [PubMed: 3010816]
25. Nguitragool W, Miller C. Inaugural article: CLC Cl^-/H^+ transporters constrained by covalent cross-linking. Proc Natl Acad Sci USA. 2007; 104:20659–20665. [PubMed: 18093952]
26. Zdebik AA, et al. Determinants of anion-proton coupling in mammalian endosomal CLC proteins. J Biol Chem. 2007; 283:4219–4227. [PubMed: 18063579]
27. DeFelice LJ, Goswami T. Transporters as channels. Annu Rev Physiol. 2007; 69:87–112. [PubMed: 17059369]
28. Miller C. A leak in the EAATs. Nat Struct Mol Biol. 2007; 14:356–357. [PubMed: 17473876]
29. Pusch M. Structural insights into chloride and proton-mediated gating of CLC chloride channels. Biochemistry. 2004; 43:1135–1144. [PubMed: 14756549]
30. Aromataris EC, Rychkov GY. ClC-1 chloride channel: matching its properties to a role in skeletal muscle. Clin Exp Pharmacol Physiol. 2006; 33:1118–1123. [PubMed: 17042925]
31. Jentsch TJ, Steinmeyer K, Schwarz G. Primary structure of *Torpedo marmorata* chloride channel isolated by expression cloning in *Xenopus* oocytes. Nature. 1990; 348:510–514. [PubMed: 2174129]

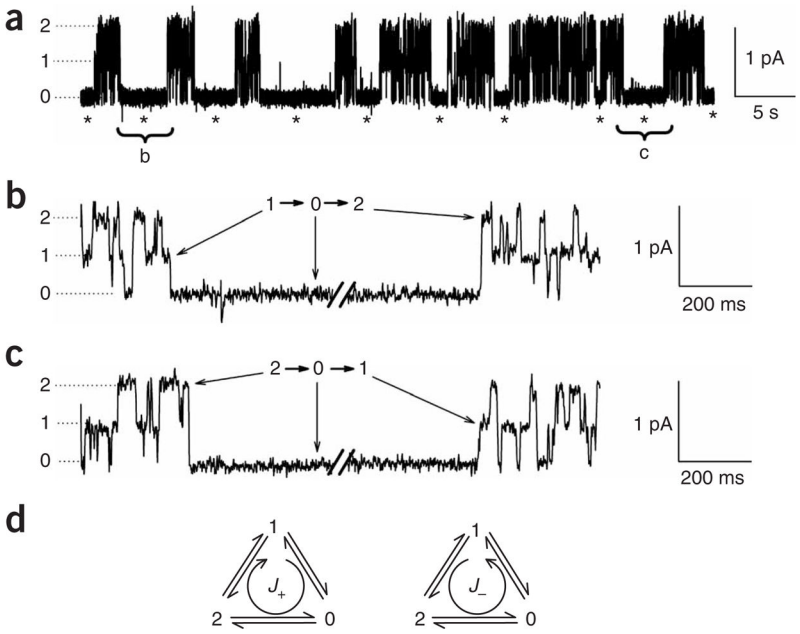

Figure 1.

ClC-0 gating. (**a**) Electrical current through a single ClC-0 channel recorded at symmetrical 120 mM Cl^-, pH_{int} 7.5, pH_{ext} 8.5 and −70 mV. Slow-gate closures are labeled with asterisks. Bursts of fast-gating events, which involve independent opening and closing of the two pores, occur between the slow-gate closures: conductance level 0, both pores closed; conductance level 1, one pore closed, one pore open; conductance level 2, both pores open. (**b**) Expanded timescale showing one of the slow-gate closures depicted in **a**. This closure involves a cycle with conductance levels ordered 1→0→2→1. We denote this as the J_+ cycle. (**c**) A slow-gate closure that proceeds in the opposite direction, with conductance levels ordered 1→2→0→1. We denote this as the J_- cycle. In addition to the asymmetrical J_+ and J_- cycles, the records contain many symmetrical slow-gate closures proceeding in the order 1→0→1 or 2→0→2 (not shown). (**d**) Diagram of the ClC-0 conductance states with the J_+ and J_- fluxes marked. The relevant '0' level is that corresponding to the long slow-gate closures (as opposed to the short 0-level events observed within bursts of fast gating).

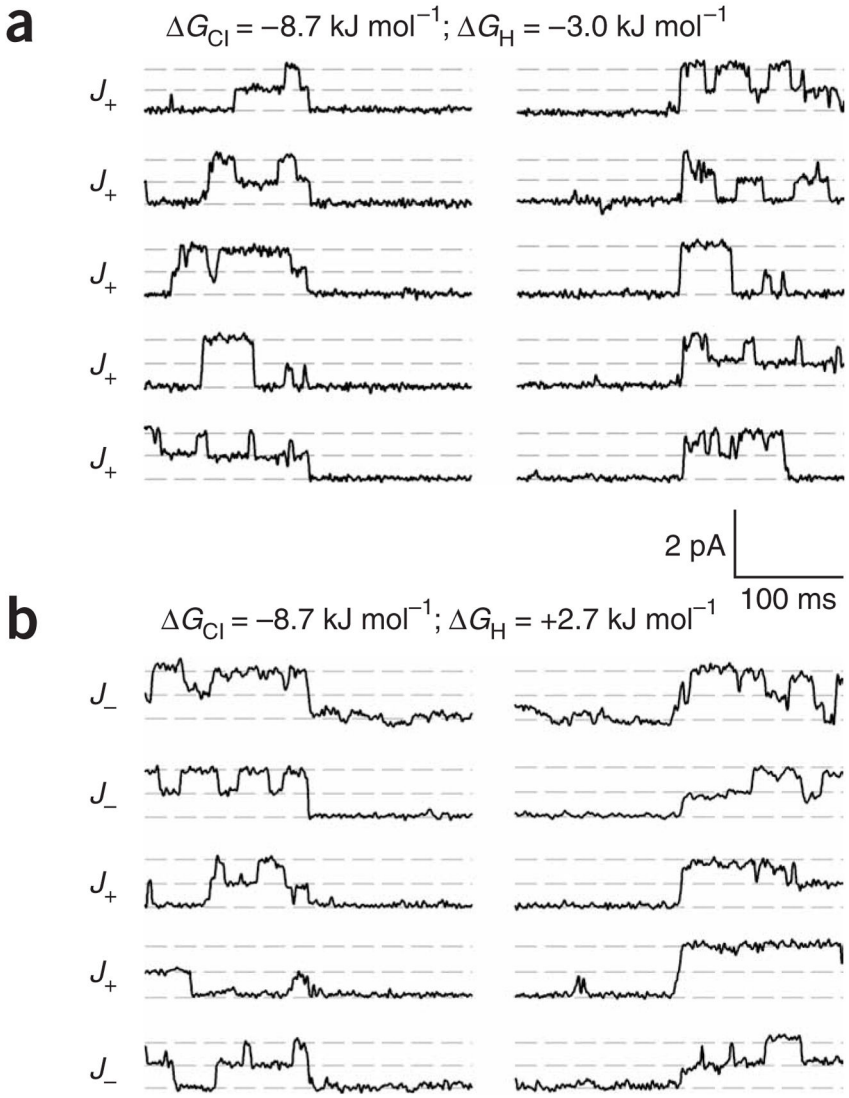

Figure 2.

Slow-gate closures recorded from patches with identical chloride gradients and different proton gradients. For each patch, the first five asymmetrical slow-gate closures are shown. For both patches, the chloride concentration was 120 mM (symmetrical) and the membrane voltage was held at −90 mV. In **a**, a one-pH-unit gradient (pH_{int} 7.5, pH_{ext} 8.5) was imposed; in **b**, a two-pH-unit gradient (pH_{int} 7.0, pH_{ext} 9.0) was imposed. The corresponding energies for the chloride and proton electrochemical gradients (ΔG_{Cl} and ΔG_H) are noted.

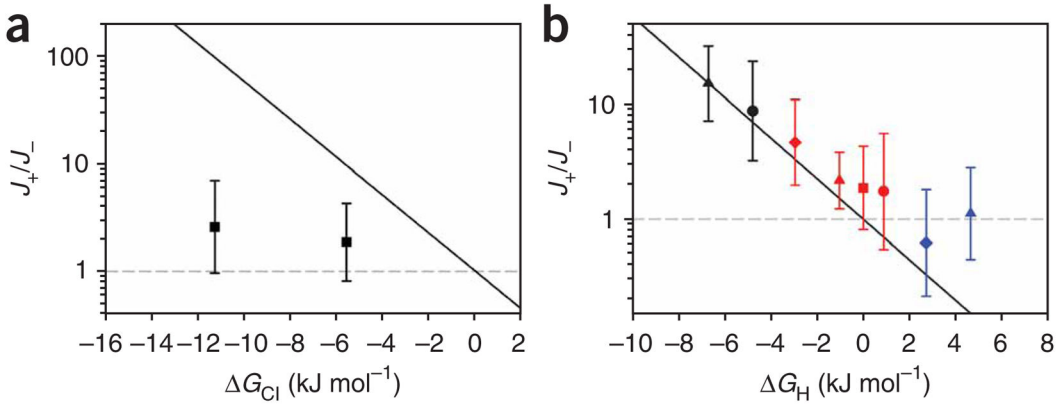

Figure 3.

The gating asymmetry ratio J_+/J_- as a function of free energy released from chloride transport, ΔG_{Cl}, and proton transport, ΔG_H. The black solid lines show the maximal expected gating asymmetry for the case in which the gating is powered by chloride transport (**a**) or proton transport (**b**). Error bars represent the 95% confidence intervals. In **b**, the different colors code for different values of pH_{ext} (black, 7.5; red, 8.5; blue, 9.5) and the different symbols represents different voltages (circles, −50 mV; squares, −58 mV; triangles, −70 mV; diamonds −90 mV). Thus, the data points represented by the same symbols (but different colors) have the same electrochemical gradients for chloride ions (but different electrochemical gradients for protons).

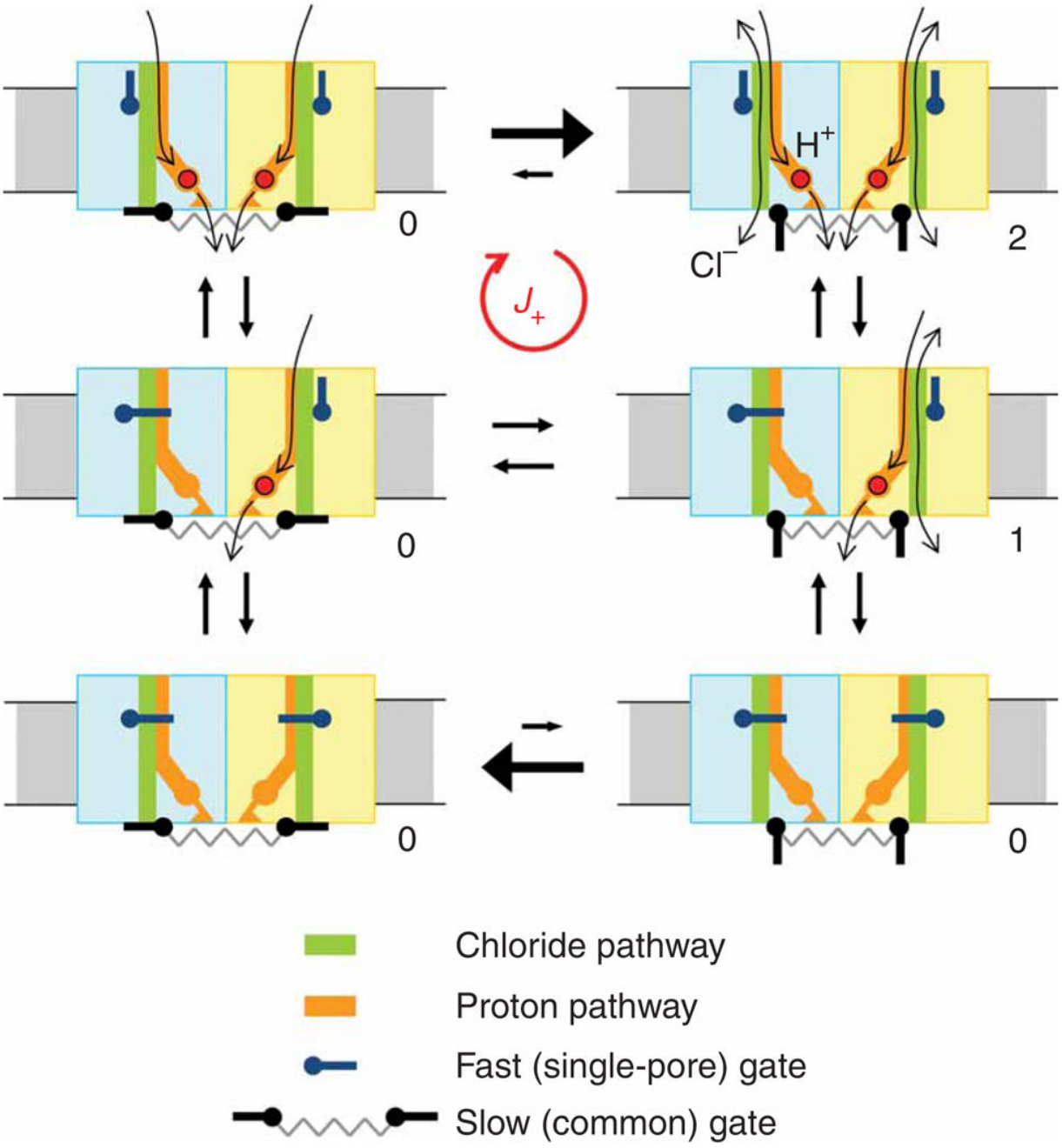

Figure 4.

A possible model for non-equilibrium gating in ClC-0. The diagrams represent ClC-0 dimers with chloride pathways (green) and proton pathways (orange). Both pathways are controlled by the fast gate (dark blue) at the extracellular side. Only the chloride pathway is gated by the slow gate (black) at the intracellular side. The slow gates within individual subunits of the dimer are coupled (gray 'spring'), such that these gates always open and close simultaneously. The number in the corner of each diagram indicates the number of open chloride pores (that is, the conductance level). The red spheres represent protons binding

inside the translocation pathway. The proton electrochemical gradient is inward (movement of protons from outside to inside is energetically downhill) and hence $J_+/J_- > 1$. In this framework, the simple assumption that binding of protons to the intracellular site favors slow-gate opening results in cycling in the J_+ direction. Experimentally, this is observed as channels more often entering the inactivated state (left-hand column) from the one-pore open state and returning from inactivation to the two-pore open state. (Note: transitions to the inactivated state directly from the level-1 state (right, middle) cannot be distinguished experimentally from those that occur from the level-0 state (right, below).) The slow gate opens more frequently when the fast gates are open because the protons can enter and bind to the activation site; the slow gate closes more frequently when the fast gates are closed because the protons escape down their electrochemical gradient.

Table 1

Gating asymmetry ratio measurements

$[Cl^-]_{ext}$ (mM)	V (mV)	ΔG_{Cl} (kJ mol^{-1})[a]	Predicted J_+/J_-	Number of patches	J_+	J_-	J_+/J_-	95% confidence interval
120	−58	−5.6	9.7	6	15	8	1.9	0.8–4.3
12	−58	−11.3	97	3	13	5	2.6	1.0–7.0
pH_{ext}	V (mV)	ΔG_H (kJ mol^{-1})[b]	Predicted J_+/J_-	Number of patches	J_+	J_-	J_+/J_-	95% confidence interval
7.50	−70	−6.7	15	8	106	7	15	7.2–32
7.50	−50	−4.8	7.0	6	35	4	8.8	3.2–24
8.50	−90	−3.0	3.3	10	28	6	4.7	2.0–11
8.50	−70	−1.0	1.5	11	37	17	2.2	1.2–3.8
8.50	−58	0	1.0	6	15	8	1.9	0.8–4.3
8.50	−50	0.8	0.70	5	7	4	1.8	0.5–5.6
9.50*	−90	2.7	0.33	4	5	8	0.6	0.2–1.8
9.50*	−70	4.6	0.15	8	9	8	1.1	0.4–2.8

(Top) Effect of the chloride electrochemical gradient at zero proton electrochemical gradient (pH_{ext} 8.5, pH_{int} 7.5, V = −58 mV, $[Cl^-]_{int}$ = 120 mM). (Bottom) Effect of the proton electrochemical gradient (at symmetrical chloride concentration $[Cl^-]_{int} = [Cl^-]_{ext}$ = 120 mM, and pH_{int} 7.50).

* One of the four patches with ΔG_H = 2.7 kJ mol^{-1} and one of the eight patches with ΔG_H = 4.6 kJ mol^{-1} was measured at pH_{int} 7.00 and pH_{ext} 9.00.

[a] ΔG_{Cl} was calculated according to equation 3.

[b] ΔG_H was calculated according to equation 2.